



HAL
open science

Development and validation of a screening system for characterizing and modeling biomass production from cyanobacteria and microalgae: Application to *Arthrospira platensis* and *Haematococcus pluvialis*

A Busnel, K Samhat, E Gérard, A Kazbar, H Marec, E Dechandol, B Le Gouic, J-L Hauser, Jeremy Pruvost

► To cite this version:

A Busnel, K Samhat, E Gérard, A Kazbar, H Marec, et al.. Development and validation of a screening system for characterizing and modeling biomass production from cyanobacteria and microalgae: Application to *Arthrospira platensis* and *Haematococcus pluvialis*. *Algal Research - Biomass, Biofuels and Bioproducts*, 2021, 58, 10.1016/j.algal.2021.102386 . hal-03609168

HAL Id: hal-03609168

<https://hal.science/hal-03609168>

Submitted on 15 Mar 2022

HAL is a multi-disciplinary open access archive for the deposit and dissemination of scientific research documents, whether they are published or not. The documents may come from teaching and research institutions in France or abroad, or from public or private research centers.

L'archive ouverte pluridisciplinaire **HAL**, est destinée au dépôt et à la diffusion de documents scientifiques de niveau recherche, publiés ou non, émanant des établissements d'enseignement et de recherche français ou étrangers, des laboratoires publics ou privés.

Development and validation of a screening system for characterizing and modeling biomass production from cyanobacteria and microalgae: Application to *Arthrospira platensis* and *Haematococcus pluvialis*

A. Busnel^{a,b}, K. Samhat^{a,c}, E. Gérard^a, A. Kazbar^b, H. Marec^a, E. Dechandol^a, B. Le Gouic^a, J.-L. Hauser^a, J. Pruvost^{a,*}

^a GEPEA, Université de Nantes, CNRS, UMR6144, Boulevard de l'Université, CRTT, BP 406, 44602 Saint-Nazaire Cedex, France

^b Algosource Technologies, Boulevard de l'Université, CRTT, BP 406, 44602 Saint-Nazaire Cedex, France

^c Platform for Research and Analysis in Environmental Sciences (PRASE), Doctoral School of Science and Technology, Lebanese University, Rafic Hariri Campus, P.O. Box 5, Hadath-Beirut, Lebanon

ARTICLE INFO

Keywords:

Photobioreactors
Screening
Modeling
Optimization
Arthrospira platensis
Haematococcus pluvialis

ABSTRACT

A miniaturized, small-scale photobioreactor (PBR) known as EOSS2-PBR (Efficient Overproducing Screening System photobioreactor) has been developed to characterize microalgal growth under controlled conditions. As with similar systems, EOSS2-PBR allows the screening of either culture conditions or species performance, but it is also specially designed to provide high levels of light absorption control conditions in the culture volume.

First, an experimental characterization was carried on to (i) determine operating conditions to adjust optimal parameters controlling EOSS2-PBR performance, such as thermal behavior of PBR, and (ii) ensure that no limitation other than light occurred to control the system and assure high reliable productivities.

EOSS2-PBR performance was then characterized by *Arthrospira platensis* and *Haematococcus pluvialis* cultures. By accurately relating growth to light transfer conditions, this facilitates the setting of kinetic growth models, which is illustrated in this work for the cyanobacterium *Arthrospira platensis*. Besides, continuous cultures of *Haematococcus pluvialis* were run in both EOSS2-PBR and 1L Airlift flat-panel PBR under the same culture conditions to confirm reliability in the determination of areal biomass productivity. Similar results were obtained in the two PBRs with a variance of less than 5%.

1. Introduction

Numerous solutions are currently being investigated to substitute chemical synthesis with biosynthesis, using plants and microorganisms to produce food, animal feed, chemicals, etc., and also to reduce the environmental impact of various processes. Microalgae, including cyanobacteria, represent a potential source of biomolecules for many different applications [1–6]. They can be found almost in every biotope of the globe, representing around 300,000 different genera. This adaptation to different environmental conditions results in the production of huge biodiversity of biomolecules (pigments, fatty acids, proteins, polysaccharides, vitamins, etc.). However, the lack of knowledge about many species and hindsight on their cultivation methods, strongly restrict the industrial potential of microalgae. Today, only around 20 microalgae species are used and commercialized at the industrial level,

for the cosmetics, animal feed and food supplement markets. A wide discrepancy exists between the number of species cultivated at an industrial scale and the great potential for microalgal biodiversity.

The production of biomass and/or molecules of interest is closely related to culture conditions and strain choice. Some species, *Arthrospira platensis* for example, will have better growth at a high pH [7]. For others, metabolites of interest will be produced in stress conditions, as with the production of beta-carotene by *Dunaliella salina* [8] and astaxanthin by *Haematococcus pluvialis* [9]. Thus, to better understand the parameters that affect biomass and metabolite production before taking them to an industrial scale, important characterization work is required at the lab scale. This is particularly the case for poorly studied and documented species, for which different culture parameters such as culture medium, light, temperature, pH, etc., must be first determined. This step is crucial in an industrial context, to determine the best cultural

* Corresponding author.

E-mail address: jeremy.pruvost@univ-nantes.fr (J. Pruvost).

conditions to achieve the best productivity and to evaluate the techno-economic and scale of production. However, this characterization step can be time-consuming [10]. In general, equipment and methods which could reduce the delay between laboratory to industrial scale would be extremely valuable.

It is well-known that there is a strong link between photoautotrophic growth and light absorption conditions, which are related to culture system geometry [11]. For example, geometry responding to a one-dimensional hypothesis such as a flat panel system, or cylindrical geometry presenting cylindrical symmetry, allows simple analytical equations to be used to represent light transfer in culture systems [12–15]. Of the numerous works using PBR geometries corresponding to the one-dimensional hypothesis for an accurate study of photosynthetic microorganism growth, we can cite Kandilian [16] and Soulies et al. [17], who investigated lipid accumulation and light spectrum effects respectively. Investigations including the modeling approach were therefore facilitated.

Screening studies to determine growth conditions are usually conducted on microplates or in Erlenmeyer flasks or serum bottles to compare medium or strain potential, with system volumes ranging from 5 mL to 4 L [18–22]. These systems, however, do not provide strict control of culture conditions, especially regarding light absorption. Recently, screening systems dedicated to photosynthetic microorganisms have been proposed, including microPHAROS™ from Xanthella and Multi-Cultivator® (MC 1000-OD) developed by Photon Systems Instruments. This latter PBR consists of eight 85 mL test tubes, can maintain an ambient temperature of up to 60 °C for all the tubes, and a sensor to monitor growth in each tube is provided. CO₂ is constantly injected by a CO₂/airflow, and a specific spectral LED light flux can be applied from 405 to 730 nm. A turbidostat mode can be held on each cultivation PBR cell. Similarly, a screening PBR named EOSS was proposed [23]. As for the Multi-Cultivator system, continuous and semi-continuous cultures are possible, but a cylindrical geometry was used in both systems with frontal illumination. As a consequence, the light transfer is not one-dimensional, which makes it difficult to determine

the light absorption conditions [10].

This work presents the design of a new screening photobioreactor named EOSS2-PBR. The main interest is to characterize and model the pairing of light absorption conditions and photosynthetic growth. The cyanobacterium *Arthrospira platensis* and the green microalga *Haematococcus pluvialis* were used in this study to demonstrate the efficiency of EOSS2-PBR. Biomass productivities obtained were compared to the predicted productivities with the kinetic growth model for *Arthrospira platensis* and experimental data from the 1 L Airlift flat-panel PBR for *Haematococcus pluvialis*.

2. Materials and methods

2.1. Experimental setup

Two types of PBR were used during this study: the EOSS2-PBR that is the basis of this work and the 1L Airlift flat-panel PBR used to validate the results obtained in EOSS2-PBR.

2.1.1. EOSS2-PBR description

EOSS2-PBR is the second version of the first screening PBR, EOSS1-PBR, which is fully described in Taleb et al. [23]. It permits screening of (i) microalgae species performance; (ii) medium composition; (iii) growth temperature; (iv) illumination conditions (continuous or day/night cycles) in reliable conditions (Fig. 1). EOSS2-PBR consists of 6 mini flat PBRs operated independently in parallel, their geometry has been modified to provide accurate control of light absorption conditions in the culture volume than on EOSS1-PBR. Each PBR is therefore constructed as a flat-panel PBR to respond to the one-dimensional hypothesis.

Each PBR has a volume of $V_r = 75$ mL ($100 \times 40 \times 20$ mm with a rounded shape at the bottom of R20 diameter) and a specific illuminated surface $a_{\text{light}} = 50$ m⁻¹ (depth of 2 cm). It is fully automated in terms of light illumination and thermoregulation, with a possibility of continuous culture. This system is made in polymethyl methacrylate

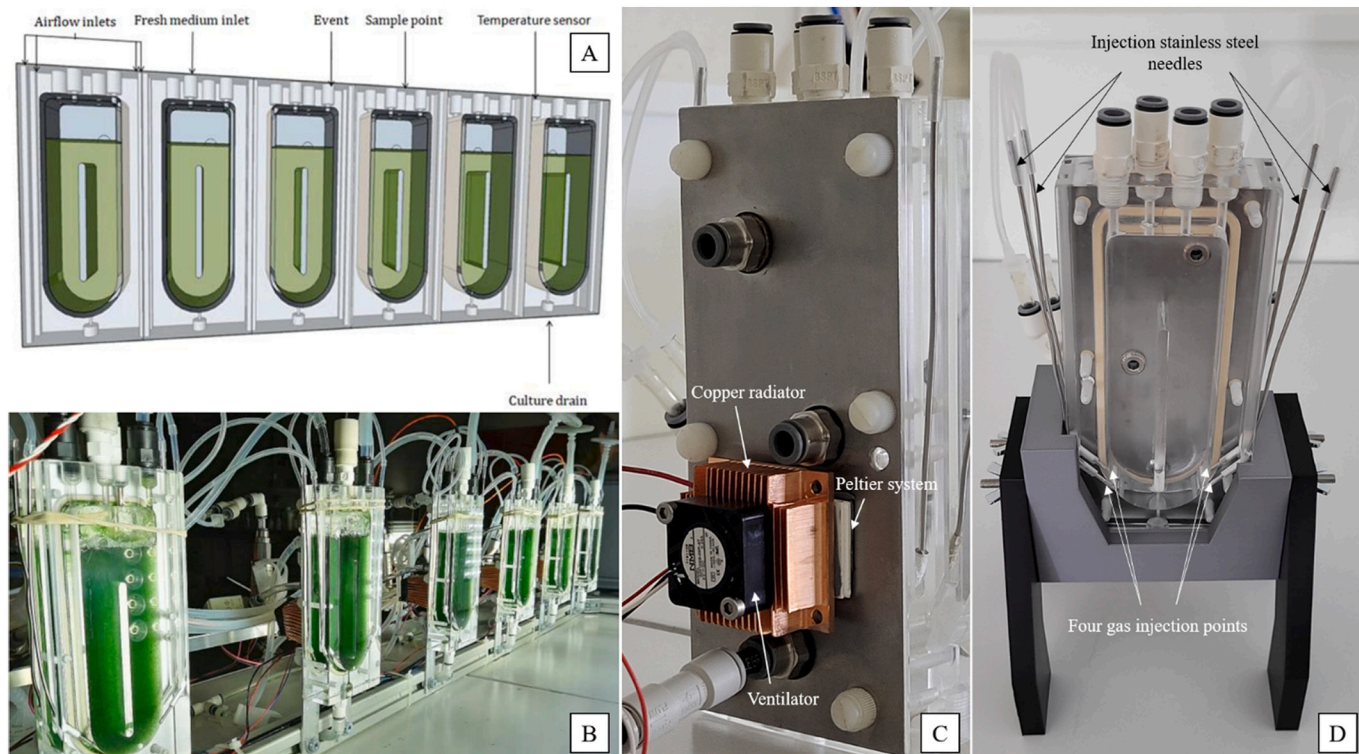


Fig. 1. Schematic representation (A) and pictures of the front (B), the backplate with the heating/cooling system (C) and the gassing system (D) of EOSS2-PBR.

(PMMA) for the transparent part (Fig. 1B) and the stainless steel backplate (Fig. 1C). A PT100 temperature sensor is used to measure and pilot a heating/cooling system composed of a Peltier system, a copper radiator, and a ventilator (Fig. 1C). Then, each dilution rate is imposed by a pump (ISMATEC® reglo ICC) to inflow fresh medium and a calibrated solenoid valve (SMC® VDW22UAH) to harvest. The calibration of the harvest solenoid valve has been done by mass of liquid measurement as a function of the opening time. A maximal error of 8% has been observed with the given harvest method. Airlift agitation is obtained by injection of air enriched in CO₂ with continuous flow maintained at 100 mL·min⁻¹ by mass flow meter/controller (EL-FLOW® Select, Bronkhorst). The gas flow has been homogeneously distributed to the 6 PBRs by 6 independent valves (Fig. 2, V1) via mixing time measurement (see Section 3.1). For optimal mixing, a 3 ways solenoid valve permits direct flux in two of four gas injection points (SMC® VDW2505G201FHQ) (Fig. 2, V2). All injection points are located at the bottom of the PBR (Fig. 1D). Two injection points are located on each side at the front part of the used volume and the two others at the background (Fig. 1D). The incident photons flux density (PFD) was provided by a set of 6 independent small white LED flat panels with light intensity ranging from 40 to 400 μmol_{hv}·m⁻²·s⁻¹ which allows either a constant or a cycled illumination intensity. Each electronic device is piloted by a program build on LabVIEW software (National Instruments, USA).

2.1.2. Airlift flat-panel PBR description

The airlift flat-panel PBR (AL-PBR) was used, in this study, to

validate the performance of EOSS2-PBR in characterizing microalgae strains performances, as represented here by the areal biomass productivity as a meaningful quantity when scaling production facilities and culture systems [13]. This AL-PBR, described in more details by Pruvost et al. [24], has a volume of $V_r = 1 \text{ L}$ ($16 \times 24.5 \times 3 \text{ cm}$) and a specific illuminated surface $a_{\text{light}} = 33.33 \text{ m}^{-1}$ (depth of 3 cm). Its non-optical rear face is made of stainless steel while its front face is constructed with transparent and non-toxic PMMA ensuring the passage of light into the PBR. PBR was set with a complete loop of common sensors and automation (Mettler Toledo M300) for microalga culture, namely pH, temperature, and gas injections (CO₂ and air). pH was regulated by automatic injection of CO₂ and temperature by ambient air blowing [24]. The incident PFD was generated by a panel of white LED, previously calibrated, which was placed vertically in front of the PBR, parallel to the optical face, to provide one-dimensional light attenuation to the PBR.

2.2. Algal strains and pre-cultivation in shake flasks

Two strains were used in this work, namely the cyanobacterium *Arthrospira platensis* (PCC8005) and the green microalga *Haematococcus pluvialis* (SAG 34-7).

Arthrospira platensis was maintained in Zarrouk medium [25] while *Haematococcus pluvialis* was maintained in a modified Bold Basal Medium (BBM) [26]. Both species were cultivated in an Erlenmeyer glass vessel and were thermo-regulated at 21 °C, stirred at 70 rpm and illuminated at 30 μmol_{hv}·m⁻²·s⁻¹ by an incubation chamber (INNOVA44®

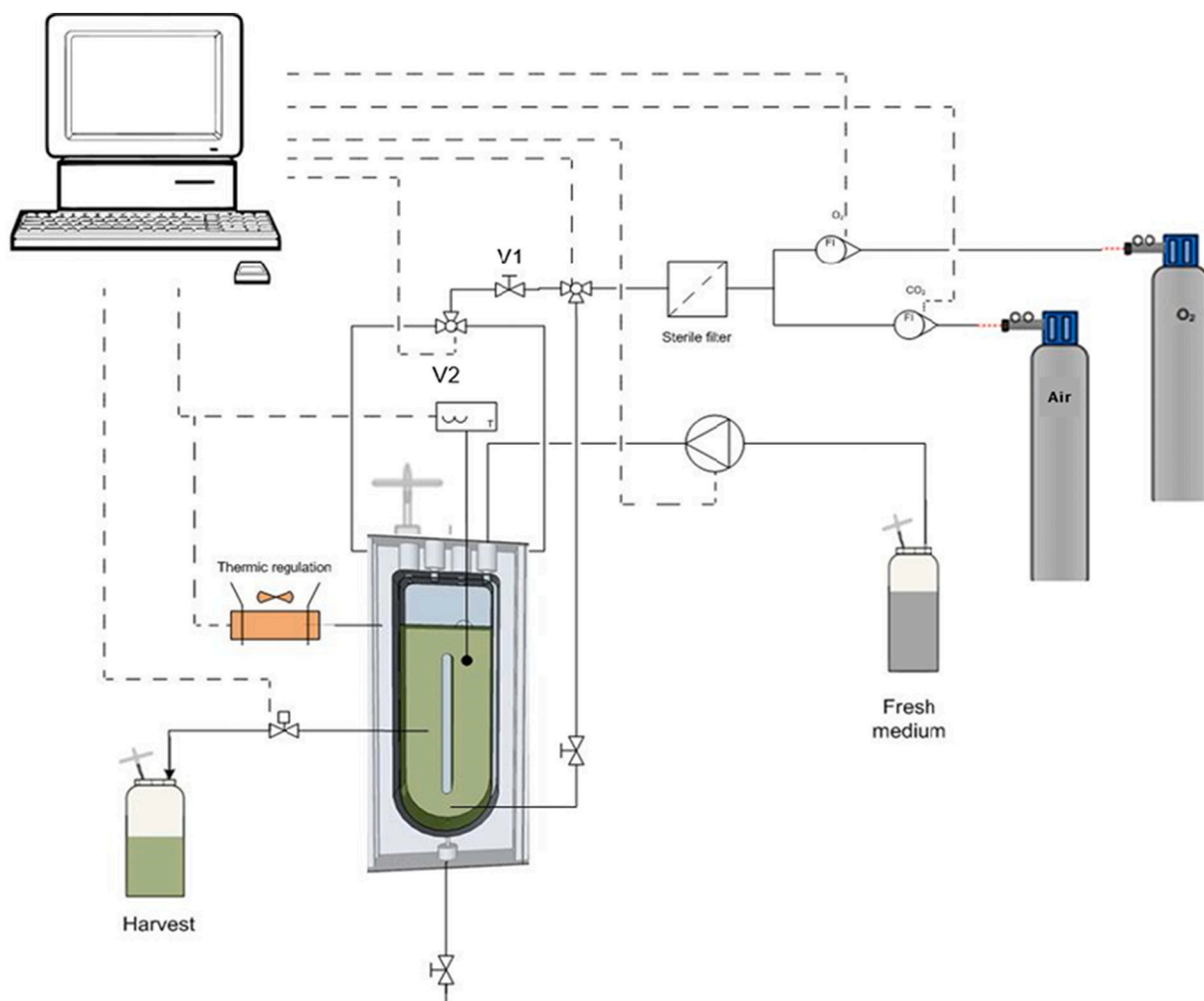


Fig. 2. Schematic of EOSS2-PBR set-up.

Incubator shaker series from New Brunswick Scientific).

2.3. Operating conditions

2.3.1. *Arthrospira platensis* cultivation in EOSS2-PBR

For *A. platensis*, EOSS2-PBR was operated at a constant temperature of 35 °C. An incident PFD of 300 $\mu\text{mol}_{\text{hv}}\cdot\text{m}^{-2}\cdot\text{s}^{-1}$ was fixed and three dilution rates of 0.011, 0.033 and 0.058 h^{-1} were applied to obtain different biomass concentrations and cover different light attenuation conditions. Air injection was enriched at 1% CO_2 to ensure a constant pH of 9.5 ± 0.3 while providing sufficient carbon to avoid growth limitation conditions.

2.3.2. *Haematococcus pluvialis* cultivation in EOSS2-PBR and airlift-PBR

H. pluvialis was cultivated in both EOSS2-PBR and AL-PBR under the same culture conditions. Cultures were run in continuous (*chemostat*) mode with optimal growth conditions (i.e., green stage). The fresh medium was injected using a dosing pump (Ismatec®), and harvesting was by overflowing into a sterilized bottle, making the reactor volume V_r constant. The temperature was maintained at 25 °C using a heating resistor connected to the transmitter probe and which is located on the rear face of the reactor. Thus, the pH is regulated by injecting CO_2 gas (2.5% CO_2) to maintain a constant pH of 7.5 ± 0.5 , the optimal pH for the growth of *H. pluvialis*, and to meet the needs in dissolved carbon to avoid growth limitation conditions. Two incident PFDs of 75 and 200 $\mu\text{mol}_{\text{hv}}\cdot\text{m}^{-2}\cdot\text{s}^{-1}$ were fixed and three dilution rates of 0.01, 0.02 and 0.03 h^{-1} were applied to investigate various light absorption conditions.

Before starting each experiment, the PBRs were sterilized for 30 min using a 5 mM peroxyacetic acid solution and rinsed twice with sterile deionized water.

2.4. Analytical methods

2.4.1. Measurement of mixing time

Determination of mixing time (t_m) in the EOSS2-PBR was performed by monitoring the conductivity of the liquid phase. The conductivity meter used was a conductometer (CD810 Tacussel, France) with a self-made probe made of two nickel wires (0.5 mm diameter 95% purity) spaced at 5 mm with an insert made by a milling machine. The end of the tube was sanded to obtain two circular wires with no glue on them. The analog output (0 V–7 V) of the conductometer was plugged into a card (USB-6009 National Instrument, USA) in the differential input.

For all experiments for mixing time measurement, distilled water was used as the liquid phase in the EOSS2-PBR, maintained at ambient temperature (21 ± 1 °C). Mixing was provided by air injection. The air was introduced at the bottom of the reactor through four (1 mm diameter) needles (two on each side, one close to the front wall, and one close to the back wall) (Fig. 1D). Air was entered from the gas circuit at a flow rate of 25 $\text{mL}\cdot\text{min}^{-1}$ and a pressure of 3.0×10^4 Pa at the bottom of each PBR (Fig. 2).

When used for cultivation, gas can be introduced alternately by the left and right needles (Fig. 1D). This guarantees good mixing on both sides of the PBR to avoid biofilm appearing on the optical surface. Since the mixing-time experiments were not conducted with microorganisms, the air was only injected on the right side. Due to the design symmetry of the PBR, the same results were achieved when using the left-side injection (data not shown).

A conductivity probe was placed in the EOSS2-PBR cell, passing by the event position (on the left of the reactor), 2.5 cm from the top of the PBR cell. The conductivity tracer consisting of 800 μL saturated salt solution (NaCl) was injected into the reactor (at time t_0), passing by the medium inlet position on the left of the reactor, also 2.5 cm from the top. Thus, NaCl solution was introduced on the opposite side to the bubbling. The injection was performed as quickly as possible to constitute a punctual perturbation. Conductivity was monitored by the

conductivity meter for 6 min, the time needed for stabilization, at the rate of one measure per second (1 Hz).

The obtained values (conductivity as a function of time) were normalized by the maximum value obtained for the experiment. Mixing time is defined as when the conductivity value exceeds 95% of the maximum value. All analyses were done in triplicate.

2.4.2. Measurement of gas-liquid mass transfer

The volumetric oxygen transfer coefficient ($k_L a$) was determined. Distilled water at ambient temperature (21 ± 1 °C) was used as the liquid phase. The dissolved oxygen concentration was monitored by an optical oxygen sensor (Pyroscience®, OXROB10) connected to Pyro oxygen logger (Pyroscience®) software. This probe took one measurement per second (1 Hz).

The medium was first deoxygenated by replacing the airflow containing oxygen with gaseous nitrogen. This step was performed until a dissolved oxygen concentration of less than 2% saturation was obtained in experimental conditions. The nitrogen flow was then turned off and replaced with airflow at the rate of 25 $\text{mL}\cdot\text{min}^{-1}$. The oxygenation step was maintained until thermodynamic equilibrium was achieved (i.e., constant dissolved oxygen concentration).

In the absence of microorganisms, the oxygen uptake rate (OUR) is equal to 0. The oxygen mass balance in the liquid phase, therefore, leads directly to the oxygen transfer rate (OTR), and the kinetics of the reoxygenation phase is governed by the following differential equation:

$$\frac{dC_L}{dt} = k_L a (C_L^* - C_L) = OTR \quad (1)$$

where C_L and C_L^* are the dissolved oxygen concentration at a given time and at equilibrium respectively. Volumetric oxygen transfer was determined by plotting $\ln\left(\frac{C_L^* - C_L}{C_L^*}\right)$ versus time, resulting in a straight line with a slope corresponding to the $k_L a$ value.

2.4.3. Characterization of thermal behavior of EOSS2-PBR

When full light attenuation occurs, microalgal culture can be considered as a black body, with a light absorption capacity close to 100% [27]. Black Indian ink was therefore used to simulate a microalgal culture for thermal behavior characterization. The aim was to determine the maximum and minimum temperatures applicable at each incident PFD by determining the corresponding cooling and heating powers. Six incident PFDs were applied to EOSS2-PBR (50, 150, 200, 300 and 400 $\mu\text{mol}_{\text{hv}}\cdot\text{m}^{-2}\cdot\text{s}^{-1}$) with a temperature set point between 5 and 50 °C for all minis PBRs. Minimal and maximal temperatures were noted when the thermic equilibrium was obtained.

2.4.4. Reproducibility evaluation

Since EOSS2-PBR consists of 6 mini PBR (named PBR cells), it was important to test their reproducibility to verify there is no significant effect in the operation of each PBR cell on the growth of microalgae. Therefore, *H. pluvialis* was cultivated in 3 PBR cells simultaneously under the same culture conditions (PFD = 100 $\mu\text{mol}_{\text{hv}}\cdot\text{m}^{-2}\cdot\text{s}^{-1}$ and $D = 0.02$ h^{-1}). The biomass productivity and the pigment contents were measured during cultivation.

2.4.5. Dry weight and biomass productivity

For both strains, the microalgal dry weight concentration C_x was determined by filtration through a pre-dried and pre-weighed glass-fiber filter (Whatman GF/F). The filters were dried for 24 h at 105 °C then weighed in triplicate. The volumetric biomass productivity P_V in the continuous cultures at dilution rate D was calculated from biomass concentration C_x measured at steady state 3 days in a row [28]. Measurements of productivities were taken in triplicate on three consecutive days. The areal biomass productivity S_x was then deduced from the specific illuminated surface a_{light} :

$$P_v = C_x D \quad (2)$$

$$S_x = P_v \frac{V_r}{S_{\text{light}}} = \frac{P_v}{a_{\text{light}}} \quad (3)$$

Note that the use of a geometry responding to the one-dimensional hypothesis facilitates the determination of areal productivity as a_{light} for flat panel PBR, obtained by:

$$a_{\text{light}} = \frac{S_{\text{light}}}{V_r} = \frac{1}{L} \quad (4)$$

where L is the depth of culture. Considering that areal biomass productivity in a light-limited condition is not dependent on the PBR geometry [13], this introduces another benefit to using such geometry to obtain meaningful quantities.

2.4.6. Pigment contents

According to Qiu et al. [29], a volume V_1 (mL) of *H. pluvialis* culture was first centrifuged at 13400 rpm for 15 min. The pellet was then suspended in a volume V (mL) of dimethyl sulfoxide (DMSO) and then incubated at 50 °C for 1–2 h in the dark until the sample turned white. After cooling, the pigment extract was diluted with a volume V_2 (mL) of 90% acetone (the ratio of DMSO: 90% acetone should be equal to 1:4) before centrifugation at 13400 rpm for 15 min. The optical density OD_λ of the supernatant was measured at 480, 630, 645, 665 and 750 nm with a UV-vis spectrophotometer (JASCO V-630). All extractions were performed in triplicates. Pigment concentrations (chlorophyll *a* (Chl-*a*), *b* (Chl-*b*) and photoprotective carotenoids (PPC)) were calculated as follows [30]:

$$\begin{aligned} C_{\text{Chl-a}} [\text{mg/L}] &= \{11.6 (OD_{665} - OD_{750}) - 1.31 (OD_{645} - OD_{750}) - 0.14 (OD_{630} - OD_{750})\} \frac{V_2}{V_1} \\ C_{\text{Chl-b}} [\text{mg/L}] &= \{20.7 (OD_{645} - OD_{750}) - 4.34 (OD_{665} - OD_{750}) - 4.42 (OD_{630} - OD_{750})\} \frac{V_2}{V_1} \\ C_{\text{PPC}} [\text{mg/L}] &= \{4.0 (OD_{480} - OD_{750})\} \frac{V_2}{V_1} \end{aligned} \quad (5)$$

where l is the cell path length (1 cm). The corresponding mass fraction of pigment “*i*” per dry weight of biomass can be estimated as $w_i = C_i / C_x$.

2.5. Theoretical considerations

2.5.1. Overview of modeling of *Arthrospira platensis* growth

If light source and PBR are planar systems, the one-dimensional hypothesis can be applied for light transfer modeling [31]. Equations

$$\frac{G_\lambda(z)}{q_{\lambda,0}} = 2 \frac{[R_d(1 + \alpha_\lambda)e^{-\delta_\lambda L} - (1 - \alpha_\lambda)e^{-\delta_\lambda L}]e^{\delta_\lambda L} + [(1 + \alpha_\lambda)e^{\delta_\lambda L} - R_d(1 - \alpha_\lambda)e^{\delta_\lambda L}]e^{-\delta_\lambda L}}{(1 + \alpha_\lambda)2e^{\delta_\lambda L} - (1 - \alpha_\lambda)^2e^{-\delta_\lambda L} - R_d(1 - \alpha_\lambda^2)e^{\delta_\lambda L} + R_d(1 - \alpha_\lambda^2)e^{-\delta_\lambda L}} \quad (11)$$

are a function of the depth of the PBR (L), so the fluence rate $G(z)$ can be determined at each point of culture depth (z), allowing calculation of the local rate of photon absorption $A(z)$. This can therefore be linked to photosynthetic growth (r_x) by introducing the kinetic growth model. For the cyanobacterium *Arthrospira platensis*, the model of Cornet et al. [32] was used:

$$r_x(z) = \rho \bar{\phi} A(z) \quad (6)$$

$$\rho = \rho_M \frac{K}{K + G(z)} \quad (7)$$

$$\bar{\phi} = M_x \bar{\phi}' \quad (8)$$

where ρ is the energy yield for photon conversion, ρ_M the maximum energy yield for photon conversion, K the half-saturation constant of photosynthesis, $\bar{\phi}$ and $\bar{\phi}'$ mass and molar quantum yields for the Z-scheme of photosynthesis respectively, and M_x the C-molar mass of biomass. For *Arthrospira platensis*, $\rho_M = 0.8$ and $\bar{\phi} = 1.85 \times 10^{-9} \text{ kg}_x \cdot \mu\text{mol}_{\text{hv}}^{-1}$ (with NO_3^{2-} as N-source) and $K = 90 \pm 5 \mu\text{mol}_{\text{hv}} \cdot \text{m}^{-2} \cdot \text{s}^{-1}$ [33].

An average biomass volumetric growth rate can then be calculated by integration over the depth of culture [13]:

$$\langle r_x \rangle = \frac{1}{L} \int_{l=0}^L r_x(z) dz \quad (9)$$

At steady state in continuous culture, $\langle r_x \rangle$ is equal to the volumetric biomass productivity of the PBR, P_v :

$$\langle r_x \rangle = P_v \quad (10)$$

Note that the areal biomass productivity S_x can be deduced from Eq. (3).

2.5.2. Modeling of light attenuation and light absorption conditions

Light attenuation through PBR ($G(z)$) is a function of (i) the technological parameters of PBR geometry and PFD and (ii) the biological parameters of biomass concentration and corresponding radiative

properties as mass absorption cross-section (Ea_λ in $\text{m}^2 \cdot \text{kg}^{-1}$), mass scattering cross-section (Es_λ in $\text{m}^2 \cdot \text{kg}^{-1}$) and backward scattering fraction ($\bar{b}_{2\lambda}$, dimensionless).

For geometries responding to the one-dimensional hypothesis, the two-flux model proved effective to properly describe light diffusion and absorption phenomena in algal suspensions. This leads to the analytical solution, as represented by [31]: where R_d represents the diffuse reflectance of the PBR back wall ($R_d = 0$ for a transparent wall) while α_λ and δ_λ are expressed as [31]:

$$\alpha_\lambda = \sqrt{\frac{Ea_\lambda}{Ea_\lambda + 2\bar{b}_{2\lambda}Es_\lambda}} \quad (12)$$

$$\delta_\lambda = C_x \sqrt{Ea_\lambda (Ea_\lambda + 2\bar{b}_{2\lambda}Es_\lambda)} \quad (13)$$

The field of fluence rate can be used to determine the local rate of photon absorption $A(z)$ which is obtained by:

$$A(z) = \frac{1}{L} \int_0^L \int_{\lambda=400}^{\lambda=700} A_{\lambda}(z) dz d\lambda = \frac{1}{L} \int_0^L \int_{\lambda=400}^{\lambda=700} E a_{\lambda} G_{\lambda}(z) dz d\lambda \quad (14)$$

Values can be then integrated over the PAR region and related to the growth kinetics (Eq. (6)). Radiative properties have already been determined for *Arthrospira platensis* in [33] ($Ea = 162 \pm 8 \text{ m}^2\text{kg}^{-1}$; $Es = 640 \pm 30 \text{ m}^2\text{kg}^{-1}$; $\bar{b}_2 = 0.03 \pm 0.002$).

Three light regimes are usually described by light attenuation conditions, as represented by fluence rates field $G(z)$: (i) full light absorption regime corresponding to " $G(z = L) < G_C$ ", (ii) luminostat regime with " $G(z = L) = G_C$ " and (iii) kinetic regime corresponding to " $G(z = L) > G_C$ ". G_C here is the fluence rate at the compensation point. It represents the minimum fluence rate with positive growth [13]. Cornet et al. [33] have shown a compensation point at $1.5 \mu\text{mol}_{\text{hv}}\cdot\text{m}^{-2}\cdot\text{s}^{-1}$ for *Arthrospira platensis*.

2.5.3. Prediction of maximal biomass productivity

Maximal biomass productivity can be predicted either by solving the overall equation model including the radiative (Eq. (10)) and kinetic growth (Eq. (5)) models or by using the simplified engineering relation proposed by Cornet et al. [33]. Maximal biomass productivity is obtained from cyanobacteria when full light absorption occurs ($G(z = L) < G_C$). The following analytical equation can be derived to obtain maximal areal biomass productivity $S_{x,\text{max}}$ [33]:

$$S_{x,\text{max}} = \rho_M \phi_{O_2} \cdot \frac{2\alpha}{1 + \alpha} \cdot \frac{K}{Ea} \cdot \ln \left[1 + \frac{q_0 Ea}{K} \right] \quad (15)$$

This formula, avoiding a complete resolution of the kinetic and radiative transfer models, was validated by Cornet et al. [33] with an overall accuracy of around 15%.

2.5.4. Statistical tests performed

Regarding the measurement replicates, all the experiences have been done in triplicates. The error has been estimated through standard deviation calculation.

All the productivities have been calculated on steady states. Dry matter and dilution rates have been measured in triplicates three days in a row after reaching a steady state.

3. Results and discussion

3.1. Mixing efficiency in EOSS2-PBR

Airflow was fixed at $100 \text{ mL}\cdot\text{min}^{-1}$ in EOSS2-PBR and distributed using a valve control in each PBR cell. Mixing time measurements were taken for each PBR cell for the first homogenized mixing at each valve control position on 6 PBR cells (Fig. 2, V1), to verify that the same mixing conditions occur in each EOSS2-PBR cell. Triplicate assays on one PBR cell highlighted a standard deviation of 15%. This standard deviation has been estimated small enough regarding the appreciation of the opening capacity of valves (manual valves with no graduation). Homogenization of mixing time was therefore carried out, accepting an error percentage of 15% between the six EOSS2-PBR cells.

As shown in Fig. 3, a mixing time of around 3.6 min was obtained for all PBR cells. Regarding biological kinetics such as doubling time (function of strains, but roughly from hours to days [34,35]), this mixing time was considered sufficiently low to assume perfectly mixed conditions. Also, the mixing time value was used as a reference to define the alternation time of lateral air injection through the 3-way solenoid valve (Fig. 2, V3). The 3-way valve permits to orientate the gas flow on the left side pipes then, a timer set at 3.6 min, switch and orientate the gas flow on the right-side pipes.

3.2. Gas-liquid mass transfer

After deoxygenation of the medium with gaseous nitrogen, airflow with oxygen was reintroduced in the EOSS2-PBR cell. The dissolved oxygen concentration increased for around 100 s before stabilizing. The corresponding $k_L a$ value was equal to 0.028 s^{-1} at $21 \pm 1 \text{ }^\circ\text{C}$ for a flow rate of $25 \text{ mL}\cdot\text{min}^{-1}$. This was higher than the $k_L a$ value reported in Pruvost et al. [36] for an intensified PBR technology presenting high volumetric productivity and its associated high oxygen production ($k_L a = 0.01 \text{ s}^{-1}$), so it was assumed that gas-liquid mass transfer performance was sufficient to consider that EOSS2-PBR has sufficient capacity to remove oxygen produced by photosynthesis and avoid its over-accumulation.

3.3. Temperature regulation efficiency

The temperature efficiency of EOSS2-PBR was tested at each PFD value to find out the limits of the system's thermoregulation. It was

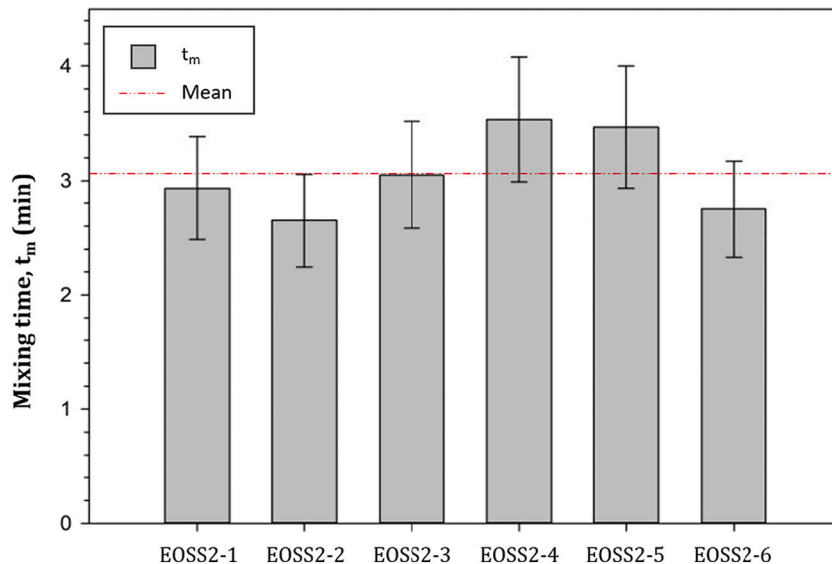


Fig. 3. Mixing time distribution across six EOSS2-PBR cells ($n = 3$).

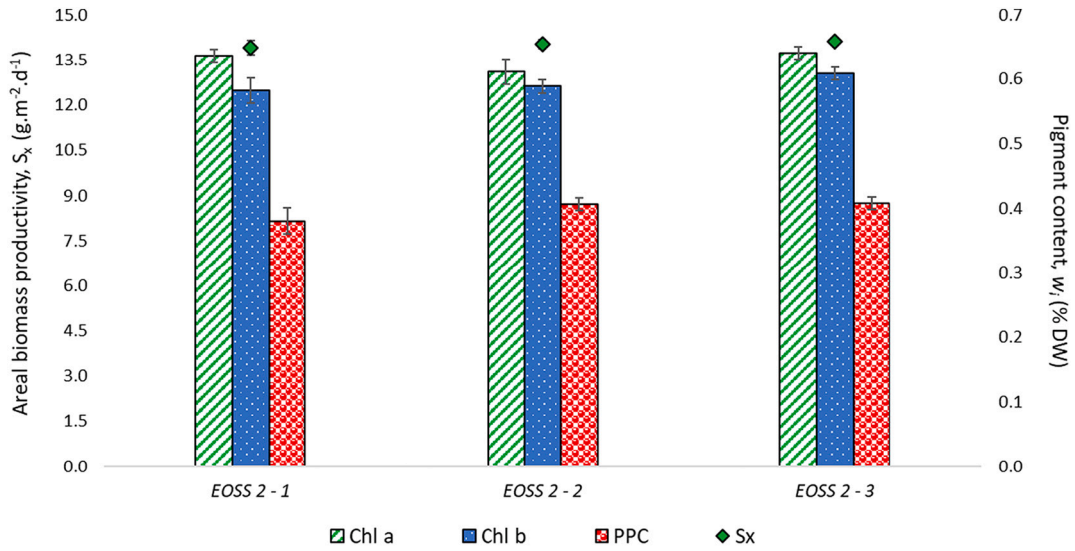


Fig. 4. Areal biomass productivities S_x , chlorophyll a concentration $C_{\text{Chl-a}}$, chlorophyll b concentration $C_{\text{Chl-b}}$ and carotenoid concentration C_{PPC} obtained in three EOSS2-PBR cells cultivating *H. pluvialis* at $\text{PFD} = 100 \mu\text{mol}_{\text{hv}}\cdot\text{m}^{-2}\cdot\text{s}^{-1}$ and $D = 0.02 \text{ h}^{-1}$.

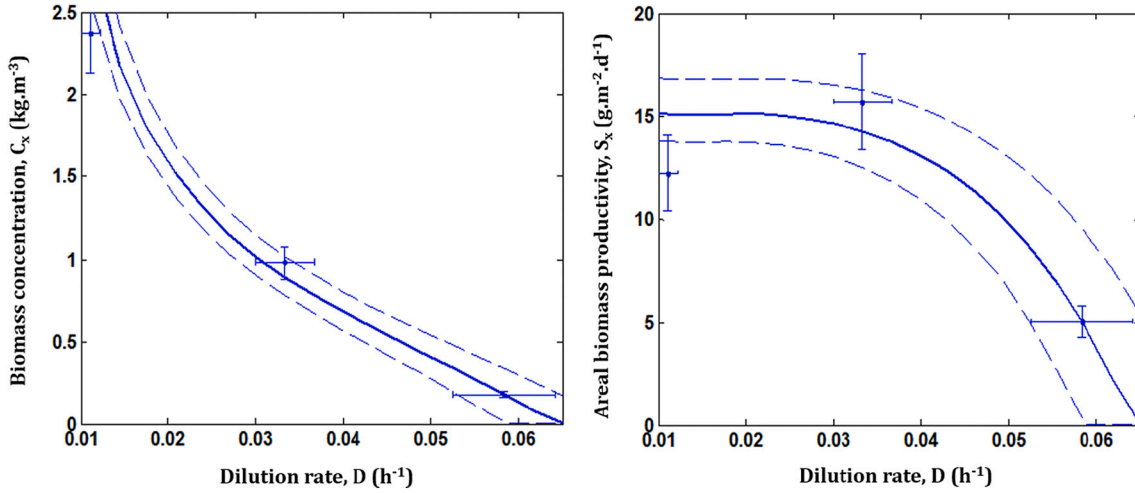


Fig. 5. Comparison between model (line) and experimental data (points) obtained by cultivating *A. pluvialis* in EOSS2-PBR. The dilution rate uncertainly has been fixed at 10% in simulations (dotted line).

found that the temperature could be stabilized at the target set points in all cases. A minimum and maximum temperature set point of respectively $5 \text{ }^\circ\text{C}$ and $50 \text{ }^\circ\text{C}$ can be maintained for a PFD from 40 to $400 \mu\text{mol}_{\text{hv}}\cdot\text{m}^{-2}\cdot\text{s}^{-1}$ in a room thermo-regulated at $20 \text{ }^\circ\text{C}$.

3.4. Reproducibility evaluation

Fig. 4 shows the areal biomass productivities and the pigment contents for *Haematococcus pluvialis* cultures in three EOSS2-PBR cells. In the same operating conditions, the difference between areal biomass productivity in the three EOSS2 cells did not exceed 5%; it was around $14.01 \pm 0.1 \text{ g}\cdot\text{m}^{-2}\cdot\text{d}^{-1}$. Similar observations can be drawn for pigment contents; in the three cells, Chl a and b content was around $1.22 \pm 0.025\%$ DW with $0.4 \pm 0.015\%$ DW of carotenoids. These results confirm that all EOSS2-PBR cells have the same performance, hence confirming the reliability of the EOSS2-PBR to screen various conditions by conducting parallel experiments in each PBR cell.

3.5. Characterization of *A. platensis* growth and comparison with growth model

Biomass productivities obtained on *Arthrospira platensis* at $300 \mu\text{mol}_{\text{hv}}\cdot\text{m}^{-2}\cdot\text{s}^{-1}$ and dilution rates of 0.011 , 0.033 and 0.058 h^{-1} are 12.2 , 15.8 and $5.0 \text{ g}\cdot\text{m}^{-2}\cdot\text{d}^{-1}$ respectively (Fig. 5). A comparison with the model prediction was added. Note that uncertainty regarding the dilution rate as fixed by the feeding pump (i.e., 10%) was considered in simulations. A correct agreement was observed. In addition to validating the model described in Cornet et al. [32] to predict the growth of *A. platensis* in PBRs, this result also demonstrates the interest of the EOSS2-PBR system for determining the kinetic constants of a growth model. For example, in the present case, the constant K which represents the half-saturation constant of photosynthesis, therefore directly related to the photosynthetic response of the strain to received light ($G(z)$), may have been obtained by adjusting the model parameter K to the experimental productivity data (using a simple regression tool such as *fmin* type in Matlab software).

Our maximal biomass productivity ($S_{x,\text{max}} = 15.84 \text{ g}\cdot\text{m}^{-2}\cdot\text{d}^{-1}$) was compared to the one predicted by the engineering formula (Eq. (15))

proposed by Cornet et al. [33]. With this equation, a theoretical value of $S_{x,max}$ of $15.93 \text{ g}\cdot\text{m}^{-2}\cdot\text{d}^{-1}$ was obtained. The discrepancy between these two results is therefore only about 3%. This confirms the interest of EOSS2-PBR as a reliable investigator of light-limited growth in a PBR.

As shown in Fig. 5, an optimal productivity of $15.84 \text{ g}\cdot\text{m}^{-2}\cdot\text{d}^{-1}$ at $300 \mu\text{mol}_{\text{hv}}\cdot\text{m}^{-2}\cdot\text{s}^{-1}$ is reached at $D = 0.033 \pm 0.003 \text{ h}^{-1}$. At higher dilution rate values, productivity decreased as far as culture washout. This has already been seen in several other works [13,14]. More surprisingly, for lower dilution rates, biomass productivity should have been found close to the maximal due to the negligible respiration activity of cyanobacteria in light [38]. As a consequence, the dark volume as obtained for low dilution rates (i.e., large biomass concentrations) has a negligible effect on the resulting PBR biomass productivity [32]. This is contradictory to our results at $D = 0.011 \pm 0.0009 \text{ h}^{-1}$, with productivity 16% lower than predicted compared to the maximal value achieved at $D = 0.033 \pm 0.003 \text{ h}^{-1}$. Such decrease could be attributed to a possible deviation in the PBR operation, as lowest dilution rate corresponds also to larger biomass concentration and longer residence time. The dilution rate $D = 0.011 \text{ h}^{-1}$ corresponds to a residence time ($=1/D$) of around 91 h. Considering the steady-state is achieved after at least 3 times the residence time value, more than 12 days were necessary to obtain the steady-state for biomass productivity measurement (25 days for $D = 0.005 \text{ h}^{-1}$). Such a long duration increases the risk of biofilm formation or operation deviation such as a drift in the feeding pump flowrate (and then dilution rate). However, such deviation could be considered acceptable (16%).

3.6. Validation of EOSS2-PBR for the determination of growth performance of *Haematococcus pluvialis* in photobioreactors

To validate the interest of using EOSS2-PBR for the determination of growth performance of strains in photobioreactors (as here represented by the areal biomass productivity), the photosynthetic growth of *H. pluvialis* was determined experimentally in both EOSS2 and AL-PBR. Cultures were conducted in chemostat mode, under 2 constant illuminations of 75 and $200 \mu\text{mol}_{\text{hv}}\cdot\text{m}^{-2}\cdot\text{s}^{-1}$ and 3 dilution rates of 0.01 , 0.02 and 0.03 h^{-1} .

According to Fig. 6, in AL-PBR, the dilution rate that maximized the productivity was 0.02 h^{-1} , yielding the highest values of areal biomass

productivity of 10.87 ± 0.18 and $24.91 \pm 0.15 \text{ g}\cdot\text{m}^{-2}\cdot\text{d}^{-1}$ for 75 and $200 \mu\text{mol}_{\text{hv}}\cdot\text{m}^{-2}\cdot\text{s}^{-1}$ respectively. Similar results were obtained with EOSS2-PBR, with maximal biomass productivities of 10.75 ± 0.22 and $25.92 \pm 0.18 \text{ g}\cdot\text{m}^{-2}\cdot\text{d}^{-1}$ reached with $D = 0.02 \text{ h}^{-1}$ for 75 and $200 \mu\text{mol}_{\text{hv}}\cdot\text{m}^{-2}\cdot\text{s}^{-1}$ respectively.

Fig. 6 summarizes the experimental values of areal biomass productivity S_x for all studied conditions in both PRBs. This confirms that, considering the standard deviations below 5% between all results, there are no significant differences in the productivities obtained for given culture conditions between both culture systems. Similar areal biomass productivities are obtained for same culture conditions (i.e., PFD and dilution rate), indicating that EOSS2-PBR can be used for the rapid determination of microalgae strain kinetics performances. For instance, using a single 1L Airlift PBR would request around one week per condition investigated, leading to around one month of culture to retrieve data to determine optimal dilution rate for a given PFD (i.e., at least 3–4 values of dilution rate are needed). With EOSS2-PBR, more data will be obtained in one week (6 dilution rates can be applied in parallel).

4. Conclusion

This work presents, for the first time, the design of a new screening photobioreactor named EOSS2-PBR. The main interest is the control of light absorption conditions (i.e., flat panel system) facilitating the characterization and modeling of the photosynthetic growth of microalgae.

EOSS2-PBR was characterized in terms of mixing and gas-liquid mass transfer performance. Both were found efficient enough to consider homogeneous nutrient concentrations in the culture and avoid dissolved oxygen accumulation, which could impair photosynthetic growth. EOSS2-PBR allows screening of culture temperature from 5 to $50 \text{ }^\circ\text{C}$.

EOSS2-PBR was proven suitable for investigating light-limited growth in photosynthetic microorganisms. This was demonstrated on the cyanobacterium *Arthrospira platensis*. Its kinetic growth model was validated through experiments. It allowed also generating quantitative data to characterize strain performances such as biomass productivity, as shown in the case of the green microalga *Haematococcus pluvialis*.

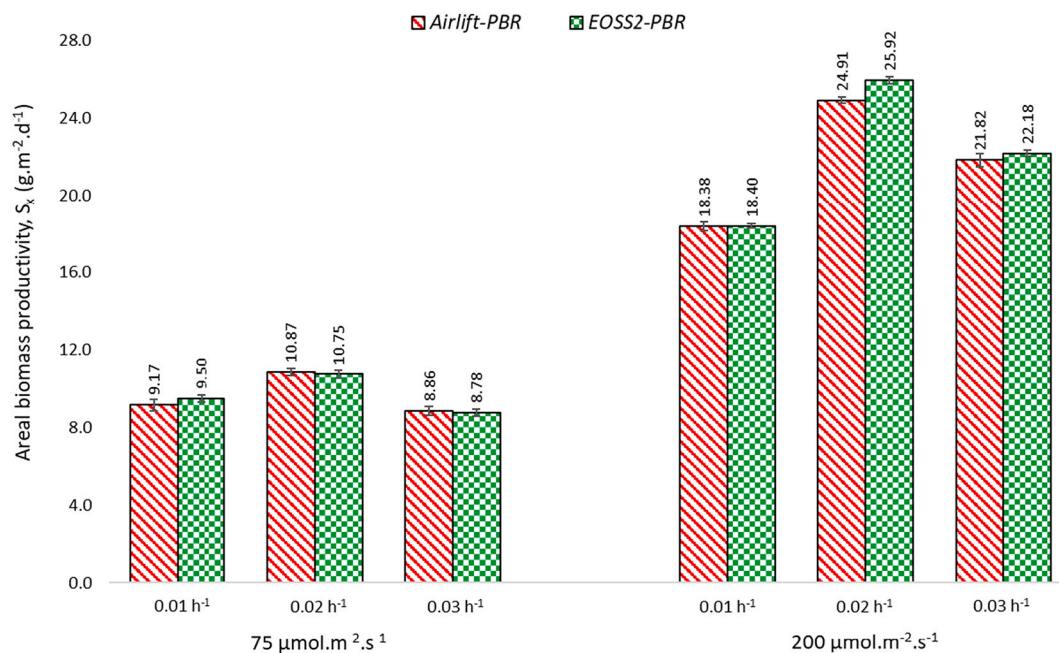


Fig. 6. Comparison of the areal biomass productivities S_x of *H. pluvialis* grown in Airlift-PBR and EOSS2-PBR at 75 and $200 \mu\text{mol}_{\text{hv}}\cdot\text{m}^{-2}\cdot\text{s}^{-1}$ as a function of dilution rates D .

Nomenclature

A	Local specific rate of photon absorption [$\mu\text{mol}_{\text{hv}}\cdot\text{kg}^{-1}\cdot\text{s}^{-1}$]
a_{light}	Specific illuminated area of photobioreactor [m^{-1}]
\bar{b}_2	Backward scattering fraction [dimensionless]
C_L	Dissolved oxygen concentration in the medium [$\text{kg}\cdot\text{m}^{-3}$]
C_L^*	Dissolved oxygen concentration at equilibrium [$\text{kg}\cdot\text{m}^{-3}$]
C_i	Concentration of pigment i [$\text{kg}\cdot\text{m}^{-3}$]
C_x	Biomass concentration [$\text{kg}\cdot\text{m}^{-3}$]
D	Dilution rate [h^{-1}]
E_a	Mass absorption cross-section [$\text{m}^2\cdot\text{kg}^{-1}$]
E_s	Mass scattering cross-section [$\text{m}^2\cdot\text{kg}^{-1}$]
G(z)	Local spherical irradiance [$\mu\text{mol}_{\text{hv}}\cdot\text{m}^{-2}\cdot\text{s}^{-1}$]
G_c	Compensation irradiance value [$\mu\text{mol}_{\text{hv}}\cdot\text{m}^{-2}\cdot\text{s}^{-1}$]
K	Half-saturation constant of photosynthesis [$\mu\text{mol}_{\text{hv}}\cdot\text{m}^{-2}\cdot\text{s}^{-1}$]
K_A	Half-saturation constant of photosynthesis [$\mu\text{mol}_{\text{hv}}\cdot\text{kg}^{-1}\cdot\text{s}^{-1}$]
K_r	Respiration inhibition constant [$\mu\text{mol}_{\text{hv}}\cdot\text{m}^{-2}\cdot\text{s}^{-1}$]
$k_{l,a}$	Volumetric oxygen transfer coefficient [s^{-1}]
L	Depth of photobioreactor [m]
M_x	C-molar mass of biomass [$\text{kg}_x\cdot\text{mol}_x^{-1}$]
P_v	Biomass volumetric productivity [$\text{kg}\cdot\text{m}^{-3}\cdot\text{d}^{-1}$]
PPFD	Photon flux density [$\mu\text{mol}_{\text{hv}}\cdot\text{m}^{-2}\cdot\text{s}^{-1}$]
q_0	Photon flux density on a given area (PPFD) [$\mu\text{mol}_{\text{hv}}\cdot\text{m}^{-2}\cdot\text{s}^{-1}$]
R_d	Diffuse reflectance of the PBR back wall [dimensionless]
r_x	Biomass volumetric growth rate [$\text{kg}\cdot\text{m}^{-3}\cdot\text{d}^{-1}$]
S_{light}	Illuminated area of photobioreactor [m^2]
S_x	Areal biomass productivity [$\text{g}\cdot\text{m}^{-2}\cdot\text{d}^{-1}$]
t	Time [days or min]
t_m	Mixing time [min]
V_r	Photobioreactor volume [m^3]
w_i	Mass fraction for pigment i in cell material [$\text{kg}\cdot\text{kg}^{-1}$ of biomass]
z	Depth of culture [m]

Greek letters

α	Linear scattering modulus [dimensionless]
δ	Extinction coefficient for the two flux model [m^{-1}]
λ	Light wavelength [nm]
ρ	Energetic yield for photon conversion [dimensionless]
ρ_M	Maximum energetic yield for photon conversion [dimensionless]
$\bar{\phi}$	Mass quantum yield for the Z-scheme of photosynthesis [$\text{kg}_x\cdot\mu\text{mol}_{\text{hv}}^{-1}$]
$\bar{\phi}'$	Molar quantum yield for the Z-scheme of photosynthesis [$\text{mol}_x\cdot\mu\text{mol}_{\text{hv}}^{-1}$]

Abbreviation

AL	Airlift
BBM	Bold Basal Medium
DMSO	Dimethyl sulfoxide
DW	Dry weight
EOSS	Efficient Overproducing Screening System
LED	Light emitting diode
OD_λ	Optical density at wavelength λ
OUR	Oxygen uptake rate
OTR	Oxygen transfer rate
PAR	Photosynthetically active radiation
PBR	Photobioreactor
PMMA	Polymethyl methacrylate
rpm	Rotation per minute
Rubisco	Ribulose-1,5-bisphosphate carboxylase/oxygenase

CRedit authorship contribution statement

- Conception and design of the work: J.Pruvost, A.Busnel
- Experimental campaign: A. Busnel, K. Samhat, E. Gérard
- Analysis and interpretation of the data: A. Busnel, K. Samhat, J. Pruvost, A. Kazbar
- Design and building of the experimental set-up: A. Busnel, H. Marec, E. Dechandol, B. Le Gouic, J-L. Hauser, J. Pruvost
- Drafting of the article: A.Busnel, K. Samhat
- Critical revision of the article for important intellectual content: J. Pruvost
- Final approval of the article: A. Kazbar, J.Pruvost

A. Busnel and E. Gérard have an equal contribution to this work based on conception, analysis and interpretation of data and drafting.

K. Samhat and A. Kazbar were involved in the conception of experiments for *Haematococcus pluvialis* and the final revision of the paper.

H. Marec, E. Dechandol, B. Le Gouic, J-L. Hauser were involved in the conception and design of EOSS2-PBR.

J. Pruvost brought a critical revision of the article and give the final approval.

Declaration of competing interest

The authors declare that they have no known competing financial interests or personal relationships that could have appeared to influence the work reported in this paper.

No conflicts, informed consent, human or animal rights applicable.

Acknowledgments

Special thanks to Atlantic Microalgae (AMI), a scientific consortium of all the establishments in the Pays de la Loire region working on microalgae and the Lebanese University (LU) that funded this study.

References

- [1] A. Muller-Feuga, "Microalgues marines: les enjeux de la recherche", sept. 1997, Consulté le: févr. 14, 2021. [En ligne]. Disponible sur: <https://archimer.ifremer.fr/doc/00000/1092/>.
- [2] A. Vonshak, *Spirulina Platensis Arthrospira: Physiology, Cell-Biology and Biotechnology*, Routledge & CRC Press, 1997. <https://www.routledge.com/Spirulina-Platensis-Arthrospira-Physiology-Cell-Biology-And-Biotechnology/Vonshak/p/book/9780748406746>.
- [3] C. Romay, J. Armesto, D. Ramirez, R. González, N. Ledon, et I. García, "Antioxidant and anti-inflammatory properties of C-phycoyanin from blue-green algae", *Inflamm. Res.*, vol. 47, n° 1, p. 36–41, janv. 1998, doi:<https://doi.org/10.1007/s000110050256>.
- [4] C. Romay, N. Ledón, et R. González, "Further studies on anti-inflammatory activity of phycocyanin in some animal models of inflammation", *Inflamm. Res.*, vol. 47, n° 8, p. 334–338, août 1998, doi:<https://doi.org/10.1007/s000110050338>.
- [5] T. Rezanka, M. Temina, A. G. Tolstikov, et V. M. Dembitsky, "Natural microbial UV radiation filters — mycosporine-like amino acids", *Folia Microbiol.*, vol. 49, n° 4, p. 339–352, juill. 2004, doi:<https://doi.org/10.1007/BF03354663>.
- [6] A. Oren et N. Gunde-Cimerman, "Mycosporines and mycosporine-like amino acids: UV protectants or multipurpose secondary metabolites?", *FEMS Microbiol. Lett.*, vol. 269, n° 1, p. 1–10, avr. 2007, doi:<https://doi.org/10.1111/j.1574-6968.2007.00650.x>.
- [7] R. A. Soni, K. Sudhakar, et R. S. Rana, "Spirulina – from growth to nutritional product: a review", *Trends Food Sci. Technol.*, vol. 69, p. 157–171, nov. 2017, doi:<https://doi.org/10.1016/j.tifs.2017.09.010>.
- [8] A. Nguyen, D. Tran, M. Ho, C. Louime, H. Tran, et D. Tran, "High light stress regimen on Dunaliella salina strains for carotenoids induction", *Integr. Food Nutr. Metab.*, vol. 3, n° 4, 2016, doi:<https://doi.org/10.15761/IFNM.1000158>.
- [9] S. Boussiba, "Carotenogenesis in the green alga *Haematococcus pluvialis*: cellular physiology and stress response", *Physiol. Plant.*, vol. 108, n° 2, p. 111–117, févr. 2000, doi:<https://doi.org/10.1034/j.1399-3054.2000.108002111.x>.
- [10] K. Loubière, E. Olivo, G. Bougaran, J. Pruvost, R. Robert, et J. Legrand, "A new photobioreactor for continuous microalgal production in hatcheries based on external-loop airlift and swirling flow", *Biotechnol. Bioeng.*, vol. 102, n° 1, p. 132–147, 2009, doi:<https://doi.org/10.1002/bit.22035>.
- [11] H. Takache, G. Christophe, J.-F. Cornet, et J. Pruvost, "Experimental and theoretical assessment of maximum productivities for the microalgae *Chlamydomonas reinhardtii* in two different geometries of photobioreactors",

- Biotechnol. Prog., vol. 26, n° 2, p. 431–440, 2010, doi:<https://doi.org/10.1002/btpr.356>.
- [12] J. Pruvost, J. F. Cornet, V. Goetz, et J. Legrand, "Modeling dynamic functioning of rectangular photobioreactors in solar conditions", *AICHE J.*, vol. 57, n° 7, p. 1947–1960, juill. 2011, doi:<https://doi.org/10.1002/aic.12389>.
- [13] J. Pruvost et J.-F. Cornet, "Knowledge models for the engineering and optimization of photobioreactors", in *Microalgal Biotechnology: Potential and Production*, C. Posten et C. Walter, Éd. De Gruyter, 2012, p. 181–224.
- [14] H. Takache, J. Pruvost, et J.-F. Cornet, "Kinetic modeling of the photosynthetic growth of *Chlamydomonas reinhardtii* in a photobioreactor", *Biotechnol. Prog.*, vol. 28, n° 3, p. 681–692, 2012, doi:<https://doi.org/10.1002/btpr.1545>.
- [15] J. Pruvost, B. Le Guic, O. Lepine, J. Legrand, et F. Le Borgne, "Microalgae culture in building-integrated photobioreactors: biomass production modelling and energetic analysis", *Chem. Eng. J.*, vol. 284, p. 850–861, janv. 2016, doi:<https://doi.org/10.1016/j.cej.2015.08.118>.
- [16] R. Kandilian, J. Pruvost, J. Legrand, L. Pilon, "Influence of light absorption rate by *Nannochloropsis oculata* on triglyceride production during nitrogen starvation", *Bioresour. Technol.* 163 (2014) 308–319.
- [17] A. Soulies *et al.*, "Investigation and modeling of the effects of light spectrum and incident angle on the growth of *Chlorella vulgaris* in photobioreactors", *Biotechnol. Prog.*, vol. 32, n° 2, p. 247–261, mars 2016, doi:<https://doi.org/10.1002/btpr.2244>.
- [18] N. Kurano, H. Ikemoto, H. Miyashita, T. Hasegawa, H. Hata, et S. Miyachi, "Fixation and utilization of carbon dioxide by microalgal photosynthesis", *Energy Convers. Manag.*, vol. 36, n° 6-9, p. 689–692, juin 1995, doi:[https://doi.org/10.1016/0196-8904\(95\)00099-Y](https://doi.org/10.1016/0196-8904(95)00099-Y).
- [19] H.-L. Yang, C.-K. Lu, S.-F. Chen, Y.-M. Chen, et Y.-M. Chen, "Isolation and characterization of Taiwanese heterotrophic microalgae: screening of strains for docosahexaenoic acid (DHA) production", *Mar. Biotechnol.*, vol. 12, n° 2, p. 173–185, avr. 2010, doi:<https://doi.org/10.1007/s10126-009-9207-0>.
- [20] E. B. Sydney *et al.*, "Screening of microalgae with potential for biodiesel production and nutrient removal from treated domestic sewage", *Appl. Energy*, vol. 88, n° 10, p. 3291–3294, 2011.
- [21] J. Van Wagenen, S. L. Holdt, D. De Francisci, B. Valverde-Pérez, B. G. Plósz, et I. Angelidaki, "Microplate-based method for high-throughput screening of microalgae growth potential", *Bioresour. Technol.*, vol. 169, p. 566–572, oct. 2014, doi:<https://doi.org/10.1016/j.biortech.2014.06.096>.
- [22] K. A. Radzun *et al.*, "Automated nutrient screening system enables high-throughput optimisation of microalgae production conditions", *Biotechnol. Biofuels*, vol. 8, n° 1, p. 65, avr. 2015, doi:<https://doi.org/10.1186/s13068-015-0238-7>.
- [23] A. Taleb *et al.*, "Development and validation of a screening procedure of microalgae for biodiesel production: application to the genus of marine microalgae *Nannochloropsis*", *Bioresour. Technol.*, vol. 177, p. 224–232, févr. 2015, doi:<https://doi.org/10.1016/j.biortech.2014.11.068>.
- [24] J. Pruvost, G. Van Vooren, G. Cogne, et J. Legrand, "Investigation of biomass and lipids production with *Neochloris oleoabundans* in photobioreactor", *Bioresour. Technol.*, vol. 100, n° 23, p. 5988–5995, déc. 2009, doi:<https://doi.org/10.1016/j.biortech.2009.06.004>.
- [25] C. Zarrouk, "Contribution à l'étude d'une Cyanophycée, influence de divers facteurs physiques et chimiques sur la croissance et la photosynthèse de "*Spirulina maxima*" (Setch et Gardner) Geitler", Thèse de doctorat, S. l. n. d., France, 1966.
- [26] H. C. Bold, "The cultivation of algae", *Bot. Rev.*, vol. 8, n° 2, p. 69–138, févr. 1942, doi:<https://doi.org/10.1007/BF02879474>.
- [27] J. Goetz *et al.*, "Photon statistics of propagating thermal microwaves", *Phys. Rev. Lett.*, vol. 118, n° 10, p. 103602, mars 2017, doi:<https://doi.org/10.1103/PhysRevLett.118.103602>.
- [28] J. Pruvost, J.-F. Cornet, et J. Legrand, "Hydrodynamics influence on light conversion in photobioreactors: an energetically consistent analysis", *Chem. Eng. Sci.*, vol. 63, n° 14, p. 3679–3694, juill. 2008, doi:<https://doi.org/10.1016/j.ces.2008.04.026>.
- [29] N. Qiu, X. Wang, et F. Zhou, "A new method for fast extraction and determination of chlorophylls in natural water", *Z. Naturforsch. C*, vol. 73, n° 1-2, p. 77–86, janv. 2018, doi:<https://doi.org/10.1515/znc-2017-0157>.
- [30] J.D.H. Strickland, T.R. Parsons, *A Practical Handbook of Seawater Analysis*, Fisheries Research Board of Canada, 1968.
- [31] L. Pottier, J. Pruvost, J. Deremetz, J.-F. Cornet, J. Legrand, et C. G. Dussap, "A fully predictive model for one-dimensional light attenuation by *Chlamydomonas reinhardtii* in a torus photobioreactor", *Biotechnol. Bioeng.*, vol. 91, n° 5, p. 569–582, 2005, doi:<https://doi.org/10.1002/bit.20475>.
- [32] J. F. Cornet, C. G. Dussap, P. Cluzel, et G. Dubertret, "A structured model for simulation of cultures of the cyanobacterium *Spirulina platensis* in photobioreactors: II. Identification of kinetic parameters under light and mineral limitations", *Biotechnol. Bioeng.*, vol. 40, n° 7, p. 826–834, 1992, doi:<https://doi.org/10.1002/bit.260400710>.
- [33] J.-F. Cornet et C.-G. Dussap, "A simple and reliable formula for assessment of maximum volumetric productivities in photobioreactors", *Biotechnol. Prog.*, vol. 25, n° 2, p. 424–435, mars 2009, doi:<https://doi.org/10.1002/btpr.138>.
- [34] N. Sakai, Y. Sakamoto, N. Kishimoto, M. Chihara, et I. Karube, "Chlorella strains from hot springs tolerant to high temperature and high CO₂", *Energy Convers. Manag.*, vol. 36, n° 6, p. 693–696, juin 1995, doi:[https://doi.org/10.1016/0196-8904\(95\)00100-R](https://doi.org/10.1016/0196-8904(95)00100-R).
- [35] M. G. De Moraes et J. A. V. Costa, "Isolation and selection of microalgae from coal fired thermoelectric power plant for biofixation of carbon dioxide", *Energy Convers. Manag.*, vol. 48, n° 7, p. 2169–2173, juill. 2007, doi:<https://doi.org/10.1016/j.enconman.2006.12.011>.
- [36] J. Pruvost, F. Le Borgne, A. Artu, et J. Legrand, "Development of a thin-film solar photobioreactor with high biomass volumetric productivity (AlgoFilm®) based on process intensification principles", *Algal Res.*, vol. 21, p. 120–137, janv. 2017, doi:<https://doi.org/10.1016/j.algal.2016.10.012>.
- [38] L. G. De La Vara et C. Gómez-Lojero, "Participation of plastoquinone, cytochrome c 553 and ferredoxin-NADP (+) oxido-reductase in both photosynthesis and respiration in *Spirulina maxima*", *Photosynth. Res.*, vol. 8, n° 1, p. 65–78, janv. 1986, doi:<https://doi.org/10.1007/BF00028477>.